行政院國家科學委員會補助專題研究計畫成果報告

※ ※※※※※※※※※※※※※※※※※※※※※※※
※
※　　膝關節病變之膝關節振動訊號的數學模式
※　　Mathematical modeling of vibration signals of knee
※　　joint in the patients with knee joint disorders
※
※
※ ※※※※※※※※※※※※※※※※※※※※※※※
※

計畫類別：☑個別型計畫　　□整合型計畫
計畫編號：NSC　89－2320－B002－109
執行期間：88 年 08 月 01 日至 89 年 07 月 31 日

計畫主持人：　　江清泉
共同主持人：　　李枝宏

本成果報告包括以下應繳交之附件：
□赴國外出差或研習心得報告一份
□赴大陸地區出差或研習心得報告一份
☑發表之論文一份
□國際合作研究計畫國外研究報告書一份

執行單位：國立台灣大學醫學院骨科

中　華　民　國　89 年　10 月 30 日

行政院國家科學委員會專題研究計畫成果報告

膝關節病變之膝關節振動訊號的數學模式

Mathematical modeling of vibration signals of knee joint in the patients with knee joint disorders

計畫編號：NSC 89-2320-B002-109

執行期限：88 年 08 月 01 日至 89 年 07 月 31 日

主持人：江清泉 國立台灣大學醫學院骨科

共同主持人：李枝宏 國立台灣大學電機工程研究所

計畫參與人員：陳甦 黃耀德 國立台灣大學電機工程研究所

一、中文摘要

關鍵詞：關節振動量測，股脛關節，退化性關節炎，數學模式，專家診斷系統

中文摘要 通道四信號量測位置位於膝蓋內側徑骨粗隆(Medial tibial bony protuberance)。

將信號分成三群(正常者、半月板無破損者和半月板破損者)，除了正常者之外，另外兩群都患有退化性膝關節炎。針對正常者、半月板無破損者和半月板破損者三群，均方根值(Root Mean Square;RMS)或是頻帶 150hz 至 1350hz 的主極點功率比都具有統計上的區別性。而正常者與半月板無破損者，在頻帶 10hz 至 500hz 的主極點功率比具有統計上的區別性。

針對半月板正常軟骨磨損的情形可以用主極點功率比區分四群(I, 2-1, 2-2, 3-3)區分的流程如圖五。針對半月板破裂軟骨磨損的情形，無法由圖五區分四群 (2-1, 2-2, 3-2, 3-3)，只有頻帶 500hz 至 750hz 的主極點功率比有區別性，且僅能區分型態 2-2 與 3-3。

Keywords: Vibration arthrometry, Femorotibial joint, Osteoarthritis, Mathematical model, Expert diagnostic system.

Abstract

The purpose of this study is to define the characteristic parameters of the vibration signals from the medial knee joint compartment of the osteoarthritic patients. Seventeen normal volunteers and 58 degenerative osteoarthritic knee patients who were scheduled to receive total knee arthroplasty were included in this study. Vibration arthrometry was performed preoperatively to every patient. The operative findings of the medial knee compartment was recorded regarding the integrity of the medial meniscus, the degree of cartilage damage of the medial femoral condyle and medial tibial plateau.

Spectral power ratio of 150 hz-1350 can be used to differentiate the integrity of the medial meniscus. For the knee with intact medial meniscus, the spectral power ratio of 10hz to 500hz is useful to differentiate the integrity of the articular cartilage.

The vibration arthrometry is an useful tool to diagnose the knee joint disorders in the medial compartment.

二、緣由與目的

研究對象

本研究的目的在探討內側股脛關節在不同膝關節病變產生之訊號。總共收集 17 位無膝關節病變之正常人，58 位退化性關節炎需要進行全人工膝關節置換的病患，這些病人都在術前接受關節聽診檢查。手術中記錄內側脛股關節面之病變，包括內側半月板有否破裂，以及股骨、脛骨關節軟骨磨損的情形(1 表示軟骨已有退化的現象，2 表示局部軟骨缺失，3 表示整片面積軟骨磨光，露出 subchondral bone。例如 2-1 型，表示內側股骨軟骨局部缺失，內側脛骨軟骨有退化現象，其他 2-2、3-2、3-

3 型依此類推)。

由術中記錄發現 58 例中，有 30 例之內側半月板破裂，28 例沒破。

實驗方法

VAM(Vibration Arthrometry signal)信號是病患在等速肌力測試儀的指引下，以 67° /Sec 的膝關節伸直彎曲運動，然後經 12bit 的數位類比轉換器，以 50khz 的取樣頻率轉成數位信號，再進行信號分析。分析的方式採 AR 模型作為振動信號的分析模型，並對信號作可適性的分割，以使信號成為區域性穩態。

軟骨型態

除了正常的軟骨，軟骨磨損型態區分為三型：型一為骨頭表面軟骨產生裂痕。型二為骨頭表面軟骨已經發生磨損，暴露軟骨下的硬骨，但部份區域的軟骨還存在。型三為骨頭表面的軟骨已經磨光。

將內側股脛骨關節面按上述軟骨型態的分類，可分成 I 型(內側股脛骨關節面股骨為型一，脛骨為正常或型一)、2-1 型(內側股脛骨關節面股骨為型二脛骨為型一)、2-2(內側股脛骨關節面股骨為型二脛骨為型二)、3-2 型(內側股脛骨關節面股骨為型三脛骨為型二)、3-3 型(內側股脛骨關節面股骨為型三脛骨為型三)。

實驗結果

(1) 均方根值(Root Mean Square;RMS)

圖一、二、三分別為正常者、半月板無破損者與半月板破損者的 VAM 訊號圖。由圖中可發現半月板破損者 VAM 訊號最大，半月板無破損者次之，正常者 VAM 訊號最小。

表一、二與表三分別為正常者、半月板正常者與半月板破損者的均方根值。正常者 RMS 平均值為 0.02075，標準差為 0.0682；半月板正常者平均值為 0.1920，標準差為 0.0577；半月板破損者平均值為 0.3499，標準差為 0.2366。

對三組進行一方分類變異數分析(one-way ANOVA)所得的 F 值為 8.1376，經查表 P 值小於 0.001。因此三個群組之間有差異性。接著再進行兩兩檢定，正常者與半月板正常者所得到的 F 值為 0.6356，P 值大於 0.05；正常者與半月板破損者所得到的 F 值為 5.6284，P 值小於 0.025；半月板正常者與半月板破損者所得到的 F 值為 11.4061，P 值小於 0.005。根據上述的結果，只要是半月板破損 RMS 可能就會比正常者與半月板正常者大，但是 RMS 無法區別正常者與半月板正常者。

(2)內部群組距離(Intraclass Distance;ID)

表四、五、六分別為正常者、半月板正常者與半月板破損者的內部群組距離。正常者的內部群組距離平均值為 0.6244，標準差為 0.0612。半月板正常者的內部群組距離平均值為 0.5961，標準差為 0.0589。半月板破損者的內部群組距離平均值為 0.5794，標準差為 0.0902。 對三組進行 ANOVA 分析，所得的 F 值為 1.9586，經查表 P 值大於 0.05，所以三組參數並無差異。

(3)主極點功率比(Spectral power ratio of dominant poles;R)

I. 演算法

利用主極點功率比當成區分參數的先決條件必須求得適當的頻帶，而在此頻帶範圍的主極點功率比又具有統計意義，既由 ANOVA 所得的 F 值大於某預設的臨界值(Theshold)。以下演算法可求得 F 值符合此臨界值的頻帶。得到的結果存於矩陣 Band Result。

```
i=1
Window=WindowDeviation
while Window<MaxBand
begin
(PowerRatio,ParameterLength)=PSD(Window);根據所給定的頻帶，計算各組的主極點功率比。有 n 組，每組長度由矩陣 L 描述
FValue=ANOVA(PowerRatio,
ParameterLength);求 n 組的 one-way ANOVA 的 F 值
If FValue>Theshold then
begin
BandResult(i)=Window
i=i+1
end
Window=Window+WindowDeviation
end
```

以下探討所使用的頻帶都是使用上述的演

算法求得。

II. 正常者、半月板正常者與半月板破損者三群

表七、八與表九分別為正常者、半月板正常者與半月板破損者的主極點功率比的分析結果。三組在頻帶 150hz 以上與 1350hz 以下具有區別性。正常者在此頻帶平均值為 7.1720，標準差為 9.8661；半月板正常者平均值為 13.2563，標準差為 15.7691；半月板破損者平均值為 25.2734，標準差為 22.8642。對三組進行 one-way ANOVA 分析，所得的 F 值為 6.045，P 值小於 0.005。因此三個群組之間有差異性。接著再進行兩兩檢定，正常者與半月板正常者所得到的 F 值為 1.9539，P 值大於 0.05；正常者與半月板破損者所得到的 F 值為 9.2281，P 值小於 0.005；半月板正常者與半月板破損者所得到的 F 值為 5.1719，P 值小於 0.05。根據上述的結果，只要是半月板破損，主極點功率比在此頻帶可能就會比正常者與半月板正常者大，但是仍舊無法區別正常者與半月板正常者。

表七、八與表九分別為正常者、半月板正常者與半月板破損者在頻帶 10hz 至 500hz 的主極點功率比的分析結果。正常者在此頻帶平均值為 5.3478，標準差為 4.2417；半月板正常者平均值為 15.0111，標準差為 15.4908；半月板破損者平均值為 16.6421，標準差為 13.5167。由表中可發現半月板正常者與半月板破損者在此頻帶主極點功率比的平均值很接近且比正常者大。正常者與半月板正常者兩組的 one-way ANOVA 的 F 值為 6.0462，P 值小於 0.025。因此正常者與半月板正常者兩群能由頻帶 10hz 至 500hz 的主極點功率比來區別。

正常者、半月板正常者和半月板破損者三群可由上述區分，圖四為區別三群的流程。接著探討軟骨磨損的情形。

III. 半月板正常

型態 I、2-1、2-2、3-3 在頻帶 200hz 至 500hz 與頻帶 750hz 至 1350hz 的主極點功率比，如表十、十一、十二、十三。型態 I 在頻帶 200hz 至 500hz 平均值為 2.7668，標準差為 0.5716；型態 2-1 平均值為 23.4811，標準差為 21.1968；型態 2-2 平均值為 4.2755，標準差為 2.0618；型態 3-3 平均值為 3.9205，標準差為 3.6489。四群主極點功率比的平均值以型態 2-1 最大，型態 2-2 與 3-3 次之，型態 I 最小。

型態 I 在頻帶 750hz 至 1350hz 平均值為 1.765，標準差為 0.2182；型態 2-1 平均值為 0.3806，標準差為 0.3071；型態 2-2 平均值為 0.1973，標準差為 0.3657；型態 3-3 平均值為 0.0857，標準差為 0.0951。四群主極點功率比的平均值以型態 I 最大，型態 2-1 與 2-2 次之，型態 3-3 最小。四群(I、2-1、2-2、3-3)在頻帶 200hz 至 500hz 與頻帶 750hz 至 1350hz 的主極點功率比利用 one-way ANOVA 所得到的 F 值分別為 5.0026、21.3136，查表所對應的 P 值分別為小於 0.01 與小於 0.001。因此四個群組之間有差異性。接著再進行兩兩檢定。各型態彼此之間兩兩檢定，所得到 F 值與 P 值的關係如表十四。型態 2-1 與 2-2、型態 2-1 與 3-3 主極點功率比在頻帶 200hz 至 500hz 具有統計上的意義，F 值分別為 6.1215、8.2116，查表所對應的 P 值分別為小於 0.05 與小於 0.025。型態 I 與 2-1 或與 2-2 或 3-3 主極點功率比在頻帶 750hz 至 1350hz 都具有統計上的意義，F 值分別為 21.6337、27.8612、284.689，查表所對應的 P 值分別為小於 0.01、0.005、0.001。

由表十四可看出，型態 I 與型態 2-1 或 2-2 或 3-3 在頻帶 750hz 至 1350hz 的主極點功率比皆有統計上的區別，故此頻帶可將四群分成兩部份，一為型態 I，另一為型態 2-1、2-2 與 3-3。而型態 2-1 與型態 2-2 或 3-3 在頻帶 200hz 至 500hz 的主極點功率比皆有統計上的區別，故此頻帶可再將三群(2-1、2-2、3-3)分成兩部份，一為型態 2-1，另一為型態 2-2 與 3-3。

型態 2-2 與 3-3 在頻帶 515hz 至 560hz。型態 2-2 在此頻帶的平均值為 0.2448，標準差為 0.1889，型態 3-3 平均值為 0.0682，標準差為 0.0961。由 one-way ANOVA 所求得的 F 值為 7.0547，查表得 $P<0.025$。

所以型態 2-2 與 3-3 可由頻帶 515hz 至 560hz 的主極點功率比區別。

綜合上述討論如圖五所示。

IV. 半月板破損

型態 2-1、2-2、3-2、3-3 在頻帶 200hz 至 500hz 與頻帶 750hz 至 1350hz 的主極點功率比，如表十八、十九、二十、二十一。型態 2-1 在頻帶 200hz 至 500hz 平均值為 7.3485，標準差為 4.3378；型態 2-2 平均值為 3.8671，標準差為 1.9478；型態 3-2 平均值為 7.4209，標準差為 7.2408；型態 3-3 平均值為 11.6491，標準差為 11.1744。四群主極點功率比的平均值以型態 3-3 最大，型態 2-1 與 3-2 次之，型態 2-2 最小。

型態 2-1 在頻帶 750hz 至 1350hz 平均值為 0.1731，標準差為 0.2156；型態 2-2 平均值為 0.6932，標準差為 1.3601；型態 3-2 平均值為 13.4655，標準差為 13.4439；型態 3-3 平均值為 7.4282，標準差為 18.3054。四群主極點功率比的平均值以型態 3-2 最大，型態 3-3 次之，型態 2-1 與 2-2 最小。

四群(2-1、2-2、3-2、3-3)在頻帶 200hz 至 500hz 與頻帶 750hz 至 1350hz 的主極點功率比，利用 one-way ANOVA 所得到的 F 值分別為 0.8835、0.4839，查表所對應的 P 值都大於 0.05。

而四群(2-1、2-2、3-2、3-3)在頻帶 500hz 至 750hz 的主極點功率比如表十八、十九、二十、二十一。型態 2-1 的平均值為 0.8099，標準差為 0.5112；型態 2-2 平均值為 29.8274，標準差為 29.747；型態 3-2 平均值為 2.8653，標準差為 2.2953；型態 3-3 平均值為 5.5315，標準差為 12.4928。其中以型態 2-2 的平均值最大，而型態 2-1 最小。利用 one-way ANOVA 所得到的 F 值為 3.5718，查表 P 值小於 0.05。各型態彼此之間兩兩檢定，只有型態 2-2 與 3-3 有區別，F 值為 8.7536，查表 P 值小於 0.01。故頻帶 500hz 至 750hz 的主極點功率比僅能區分型態 2-2 與 3-3。所以半月板破損後無法利用圖五流程區分，必須重新設定頻帶。

受到半月板破裂的引響或是病例數不夠，導致四群(2-1、2-2、3-2、3-3)當中，只能找出和型態 3-3 有區別的頻帶。

型態 2-1、3-3 在頻帶 260hz 至 360hz 的主極點功率比如表二十二、二十三。型態 2-1 的平均值為 6.3397，標準差為 4.233；型態 3-3 平均值為 1.5338，標準差為 1.2785，利用 one-way ANOVA 所得到的 F 值為 14.6371，查表 P 值小於 0.001。

型態 2-2、3-3 在頻帶 480hz 至 580hz 的主極點功率比如表二十四、二十五。型態 2-2 的平均值為 9.3466，標準差為 7.627；型態 3-3 平均值為 1.6403，標準差為 2.8683，利用 one-way ANOVA 所得到的 F 值為 11.9972，查表 P 值小於 0.005。

型態 3-2、3-3 在頻帶 760hz 至 935hz 的主極點功率比如表二十六、二十七。型態 3-2 的平均值為 13.4623，標準差為 13.4437；型態 3-3 平均值為 0.9602，標準差為 2.8751，利用 one-way ANOVA 所得到的 F 值為 10.7892，查表 P 值小於 0.005。

結論與討論

正常者和半月板破損者、半月板正常者和半月板破損者，不論是 RMS 或是在頻帶 150hz 至 1350hz 的主極點功率比都具有統計上的區別性，然而 RMS 無法區別正常者和半月板正常者，必須改採頻帶 10hz 至 500hz 的主極點功率比，才具有統計上的區別性。

無論半月板是否破損，皆含程度不一的軟骨磨損，半月板正常時，型態 I、2-1、2-2、3-3 四群能由圖五的流程予以區分，但是半月板破損後，能量的分佈改變，原來的頻帶不再適用。頻帶 500hz 至 750hz 的主極點功率比，四群雖然有統計上的區別，然而僅能區分型態 2-2 與 3-3。

振動訊號的來源，是由於軟骨的磨損造成骨頭表面的不平滑，因而膝關節快速擺動時產生振動訊號，此訊號能量集中在 500hz 以下。而半月板破損之後，型態 2-1 能量集中的頻帶與半月板正常者無異，都是集中在頻帶 200hz~500hz，型態 2-2 能量會往 500hz~750hz 集中，型態 3-3 能量會往 200hz~500hz 集中。所以半月板破損後能量分佈會隨軟骨磨損的型態不同，而反映在不同的頻帶，因此無法利用圖五。而

且可能是病例數不夠，重新設定頻帶只能找出可以區分型態 2-1 與 3-3、2-2 與 3-3 或是 3-2 與 3-3 的頻帶。

三、參考文獻

1. Bellanger MG: Adaptive digital filters and signal analysis. Marcel Dekker, Inc., 1987.

2. Beverland DE, McCoy GF, Kernohan WG, Mollan RAW: What is patellofemoral crepitus? J Bone Joint Surg 68B:496, 1986.

3. Chu ML, Gradisar IA, Railey MR: Detection of knee joint diseases using acoustical pattern recognition technique. J Biomech 9:111-4,1976.

4. Chu ML, Gradisar IA, Zavodney LD: Possible clinical application of a noninvasive monitoring technique of cartilage damage in pathological knee joints. J Clin Eng 3:19-27,1978.

5. Giordano AA and Hsu FM: Least square estimation with applications to digital signal processing, 1985.

6. Haykin S: Adaptive filter theory, Prentice-Hall, 1996.

7. Jiang CC, Liu YJ, et al: Physiological patellofemoral crepitus in knee joint disorders. Bulletin Hosp for Joint Diseases 53:7-11, 1994.

8. Jiang CC, Liu YJ, et al: Vibration arthrometry of the knee with torn meniscus: A preliminary report. J Formos Med Assoc 93:622-5, 1994.

9. Jiang CC, Liu YJ, et al: Vibration arthrometry for the diagnosis of meniscal tear of the knee. J Orthop Surg ROC 12:1-5, 1995.

10. 江清泉、劉益瑞等：膝關節病變的髕骨振動。 J of Applied Biomech. 9:78-83,1994.

11. Kay SM: Moden spectral estimation: Theory and applications,1988.

12. Kernohan WG, Beverland DE, McCoy GF, Hamilton A, Watson P, Mollan RAB: Vibration arthrometry. A preview. Acta Orthop Scandinavica 1:70-9,1990.

13. Liu YR, Jiang CC, Fu SE, et al: Vibration arthrography of the knee joint disorders. Biomed Eng-Appl Basis Comm 5:53-60,1993.

14. McCoy GF, McCrea JD, Beverland DE, Kernohan WG, Mollan RAB: Vibration arthrography as a diagnostic aid in diseases of the knee. J Bone Joint Surg [Br] 69:288-293, 1987.

15. McCrea JD, McCoy GF, Kernohan WG, McClelland CJ, Mollan R: Moderne tendenzen in der phonoarthrographie. Z Orthop 123:13-17,1985.

16.McCrea JD, McCoy GF, Kernohan WG, McClelland CJ, Mollan R: Vibrationarthrographie in der diagnostik von kniegelenkskrankheiten. Z Orthop 123:18-22,1985.

17.Mollan RAB, McCullagh, GC: A critical appraisal of auscultation of human joints. Clinical Orthopaedics and Related Research. 170:231-237,1982.

18.Mollan RAB, Kernohan GW, Watters PH: Artefact encountered by the vibration detection system. J Biomechanics 16:193-199,1983.

19.Moussavi ZMK, Rangayyan RM, et al: Screening of vibroarthrographic signals via adaptive segmentation and linear prediction modeling. IEEE Transactions on Biomed. Engineering 43:15-23,1996.

20.Neely LA, Kernohan WG, Barr DA, Mee CHB, Mollan RAB: Optical measurements of physiological patellar crepitus. Clin Phys Physiol Meas 12:219-226,1991.

21.Oehl R, Bohnenberger J, Heinkelmann W: Zur Technil der phonoarthorographie. Med Welt 25:1984-9,1974.

22.Oppenheim AV, Schafer RW: Discrete-time signal processing. Prentice-Hall, Englewood Cliffs, New Jersey, 1989.

23.Rangayyan F, et al: Analysis of knee joint sound signals for noninvasive diagnosis of cartilage pathology. IEEE EMB Magazine 65-68,1990.

24.Shen Y, Rangayyan RM, et al: Localization of knee joint cartilage pathology by multichannel vibroarthrography. Med. Eng. Phys 17:583-594, 1995.

25.Strobel M, Stedtfeld HW: Diagnostic evaluation of the knee. Springer-Verlag Berlin, Heidelberg, 1990.

26.Tavathia S, Rangayyan RM, Frank CB, Bell GD, Ladly KO, Zhang YT: Analysis of knee vibration signals using linear prediction. IEEE Transactions on Biomedical Engineering 39:959-969,1992.

27.Therrien CW : Discrete random signals and statistical signal processing, Prentice-Hall, 1992.

28.Zhang YT, Ladly KO, Rangayyan RM, Frank CB, Bell GD, Liu ZQ: Muscle contraction interference in acceleration vibrathrography, proc. The 12thIEEE Eng. Med. Bio. Sco. Cong., pp2150-2151, Pennsylvania, USA, Nov.,1990.

29.Zhang YT, Rnagayyan RM, Frank CB, Bell GD, Ladly KO, Liu ZQ: Classificaiton of knee sound signals by using neural network: Preliminary study., Proc. of the Lasted International Symposium of Expert System and Neural Network, pp61-62, Honolulu, Hawaii, Aug., 1990.

30. Zhang YT, Frank CB, Rangayyan RM, Bell GD: Mathematical modeling and spectrum analysis of the physiological patello-femoral pulse train produced by slow knee movement. IEEE Transactions on Biomedical Engineering 39:971-979,1992.

31. Moussavi Zahra MK,Rangayyan RM,Bell GD,Frank CB,Ladly KO,Zhang
YT:Screen of Vibroarthrographic Signals via Adaptive Segmentation and Linear Prediction Modeling.IEEE Transactions on Biomedical Engineering 43:15-23,1996

32. Jiang CC, Lee JH, Yuan TT: Vibration Arthrometry in the Patients with Failed Total Knee Replacement. IEEE Trans. Biomed Eng 47:219-227, 2000

33. Lee JH, Jiang CC, Yuan TT: Vibration arthrometry in the Patients with Knee Joint Disorders. IEEE Trans. Biomed Eng 47:1131-3, 2000

圖一 正常者的 VAM 訊號

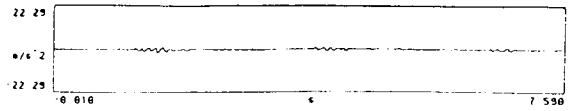

圖二半月板無破損者的 VAM 訊號

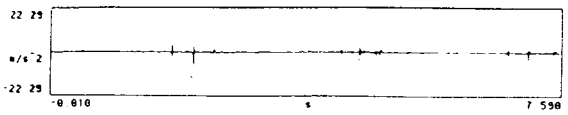

圖三半月板破損者的 VAM 訊號

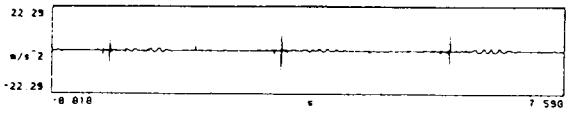

圖四 區別三群的流程

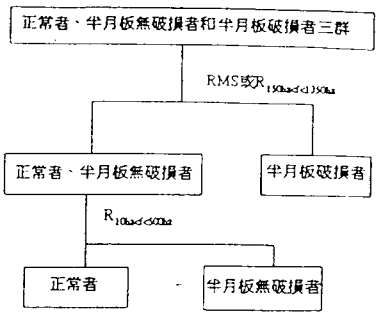

圖五 區別半月板正常時四群的流程

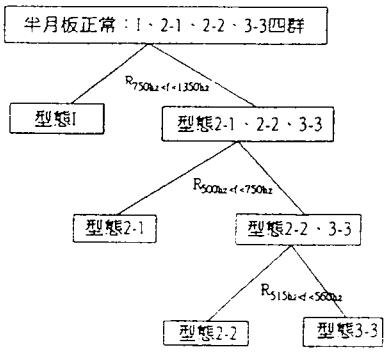

表一正常者的均方根值

編號	RMS 值
1	0.2340
2	0.1635
3	0.1441
4	0.1916
5	0.1314
6	0.1177
7	0.2474
8	0.1527
9	0.2586
10	0.1593
11	0.2539
12	0.1533
13	0.4027
14	0.2789
15	0.2045
16	0.2301
17	0.2038
平均值	0.2075
標準差	0.0682

表二半月板無破損者的均方根值

編號	RMS 值
1	0.1407
2	0.2048
3	0.1963
4	0.1387
5	0.1678
6	0.2669
7	0.2057
8	0.3064
9	0.1571
10	0.2366
11	0.1636
12	0.2085
13	0.1205
14	0.1438
15	0.1730
16	0.1586
17	0.3050
18	0.1212
19	0.0709
20	0.2009
21	0.2550
22	0.1909
23	0.1504
24	0.2166
25	0.2455
26	0.2247
27	0.1255
28	0.2800
平均值	0.1920
標準差	0.0577

表三半月板破損者的均方根值

編號	RMS 值
1	0.8528
2	0.2024
3	0.2582
4	0.1558
5	0.1900
6	0.2211
7	1.3930
8	0.4036
9	0.2049
10	0.4522
11	0.3972
12	0.2534
13	0.1868
14	0.3154
15	0.4155
16	0.2427
17	0.3514
18	0.3026
19	0.4654
20	0.4153
21	0.3647
22	0.4648
23	0.1921
24	0.2805
25	0.2203
26	0.2637
27	0.2742
28	0.1441
29	0.3130
30	0.2994
平均值	0.3499
標準差	0.2366

表四正常者的內部群組距離

編號	ID
1	0.5440
2	0.6792
3	0.6107
4	0.6593
5	0.7352
6	0.6271
7	0.5780
8	0.6433
9	0.5842
10	0.5561
11	0.6217
12	0.7467
13	0.6598
14	0.5995
15	0.6725
16	0.5735
17	0.5249
平均值	0.6244
標準差	0.0612

表五半月板無破損者的內部群組距離

編號	ID
1	0.6443
2	0.6609
3	0.6417
4	0.6620
5	0.5492
6	0.5377
7	0.5778
8	0.6015
9	0.6552
10	0.5829
11	0.5523
12	0.5990
13	0.5057
14	0.6488
15	0.5486
16	0.5923
17	0.5486
18	0.6187
19	0.6433
20	0.5524
21	0.6964
22	0.6647
23	0.6112
24	0.5007
25	0.4904
26	0.5173
27	0.5855
28	0.7007
平均值	0.5961
標準差	0.0589

表六半月板破損者的內部群組距離

編號	ID
1	0.5293
2	0.5752
3	0.7648
4	0.6685
5	0.5325
6	0.5442
7	0.3273
8	0.6248
9	0.6544
10	0.4848
11	0.4456
12	0.6259
13	0.5442
14	0.5907
15	0.6826
16	0.6340
17	0.7233
18	0.5516
19	0.5548
20	0.6937
21	0.5289
22	0.4911
23	0.5513
24	0.5140
25	0.7172
26	0.6098
27	0.4952
28	0.5691
29	0.5373
30	0.6155
平均值	0.5794
標準差	0.0902

表七正常者的主極點功率比

編號	$R_{150Hz\ \sim\ 1350Hz}$ (%)	$R_{1040Hz\ \sim\ 3000Hz}$ (%)
1	3.4802	2.8876
2	8.7572	6.0686
3	15.8001	14.9420
4	3.7240	5.9458
5	8.4183	9.0720
6	7.2392	8.3663
7	1.6019	1.5041
8	3.0144	3.4084
9	1.5678	2.7366
10	11.4084	13.0122
11	43.2401	2.1424
12	1.5295	1.6672
13	0.7370	1.2563
14	1.4820	1.5486
15	2.5621	3.1138
16	4.3624	10.8976
17	2.9992	2.3434
平均值	7.1720	5.3478
標準差	9.8661	4.2417

表八半月板無破損者的主極點功率比

編號	$R_{150Hz\ \sim\ 1350Hz}$ (%)	$R_{1040Hz\ \sim\ 3000Hz}$ (%)
1	5.8077	6.2235
2	7.5874	5.5341
3	8.8765	5.9489
4	84.9080	56.7166
5	38.3658	43.4785
6	6.9733	9.7640
7	2.8914	3.3266
8	8.4841	8.6333
9	4.1194	30.1180
10	18.9756	4.4038
11	5.6453	17.7960
12	10.2280	5.8040
13	10.9784	12.3684
14	14.5101	14.4392
15	11.9588	3.4992
16	14.3207	14.7315
17	2.3265	5.2377
18	3.5653	4.8952
19	3.4441	5.0276
20	25.0793	9.0666
21	10.0790	65.2082
22	17.0351	18.0105
23	16.6840	21.4688
24	14.0944	7.4680
25	4.6892	11.3308
26	11.1747	17.6896
27	4.5460	5.3257
28	3.8275	6.7978
平均值	13.2563	15.0111
標準差	15.7691	15.4908

表九半月板破損者的主極點功率比

編號	$R_{150Hz<f<1350Hz}$ (%)	$R_{1040Hz<f<3000Hz}$ (%)
1	75.3541	21.9246
2	39.1714	30.5414
3	11.2525	9.7846
4	22.7117	4.4648
5	10.4581	11.1684
6	5.0879	17.1683
7	0.0037	1.8164
8	39.0306	11.0737
9	31.2213	38.2413
10	46.7317	14.7015
11	12.0331	11.9760
12	39.7251	22.7083
13	20.3000	23.0655
14	15.7409	19.1939
15	48.2359	48.4587
16	21.6585	56.3172
17	15.0758	17.1302
18	19.1023	23.8615
19	52.0719	14.0029
20	11.5958	13.3762
21	32.2666	36.1422
22	3.1127	9.3111
23	1.8153	3.8351
24	12.4923	12.0379
25	78.7007	2.0024
26	2.5447	3.0187
27	3.6836	2.9013
28	5.6334	4.0312
29	3.3548	10.3826
30	78.0343	4.6261
平均值	25.2734	16.6421
標準差	22.8642	13.5167

表十.半月板正常：型態 1 的主極點功率比

編號	$R_{200Hz<f<500Hz}$ (%)	$R_{500Hz<f<750Hz}$ (%)	$R_{750Hz<f<1350Hz}$ (%)	$R_{1350Hz<f<5600Hz}$ (%)
1	2.1951	1.3382	1.9832	0.0243
2	3.3384	2.0567	1.5468	0.7279
平均值	2.7668	1.6974	1.7650	0.3761
標準差	0.5716	0.3593	0.2182	0.3518

表十一.半月板正常：型態 2-1 的主極點功率比

編號	$R_{200Hz<f<500Hz}$ (%)	$R_{500Hz<f<750Hz}$ (%)	$R_{750Hz<f<1350Hz}$ (%)	$R_{1350Hz<f<5600Hz}$
1	3.8990	3.5436	0.1158	0.4273
2	55.4243	27.9529	0.5841	0.0404
3	29.8901	0.6147	0.7745	0.0571
4	4.7111	0.1780	0.0480	0.0000
平均值	23.4811	8.0723	0.3806	0.1312
標準差	21.1968	11.5508	0.3071	0.1722

表十二.半月板正常：型態 2-2 的主極點功率比

編號	$R_{200Hz<f<500Hz}$ (%)	$R_{500Hz<f<750Hz}$ (%)	$R_{750Hz<f<1350Hz}$ (%)	$R_{1350Hz<f<5600Hz}$ (%)
1	2.4892	0.0525	0.0830	0.0012
2	6.1125	1.5480	0.2037	0.5123
3	2.4589	0.3253	0.0037	0.1381
4	2.9133	14.5724	1.2202	0.2851
5	4.0698	0.5608	0.0697	0.0617
6	4.6056	5.1711	0.0528	0.0178
7	8.9178	0.4841	0.0742	0.2764
8	4.7780	2.5071	0.0612	0.4896
9	2.1349	9.4428	0.0071	0.4215
平均值	4.2755	3.8516	0.1973	0.2448
標準差	2.0618	4.7620	0.3657	0.1889

表十三.半月板正常：型態 3-3 的主極點功率比

編號	$R_{200Hz<f<500Hz}$ (%)	$R_{500Hz<f<750Hz}$ (%)	$R_{750Hz<f<1350Hz}$ (%)	$R_{1350Hz<f<5600Hz}$ (%)
1	1.8925	0.1755	0.0054	0.0378
2	2.6316	0.2751	0.0434	0.0570
3	2.5789	0.3160	0.0503	0.0858
4	4.2785	17.9457	0.2589	0.3576
5	6.4010	0.9927	0.2200	0.1460
6	1.9980	1.5772	0.0117	0.0241
7	14.9622	0.0403	0.0000	0.0048
8	4.2251	8.7896	0.0871	0.0631
9	1.0215	0.1234	0.2514	0.0013
10	1.3922	3.5469	0.0746	0.0000
11	4.0667	0.1026	0.0108	0.0253
12	1.5980	0.3562	0.0150	0.0161
平均值	3.9205	2.8534	0.0857	0.0682
標準差	3.6489	5.1479	0.0951	0.0961

表十四半月板正常　型態 1、2-1、2-2、3-3 彼此之間兩兩檢定，F 值與 P 值的關係表

半月板正常		$R_{200Hz<f<500Hz}$ (%)	$R_{750Hz<f<1350Hz}$ (%)
(1,2-1)	F 值	1.2729	21.6337
	P 值	>0.05	<0.01
(1,2-2)	F 值	0.8616	27.8612
	P 值	>0.05	<0.005
(1,3-3)	F 值	0.1707	284.689
	P 值	>0.05	<0.001
(2-1,2-2	F 值	6.1215	0.6472
	P 值	<0.05	>0.05
(2-1,3-3	F 值	8.2116	7.5168
	P 值	<0.025	<0.025
(2-2,3-3	F 值	0.0622	0.9269
	P 值	>0.05	>0.05

表十五正常者的主極點功率比

編號	$R_{200Hz<f<500Hz}$ (%)	$R_{500Hz<f<750Hz}$ (%)	$R_{750Hz<f<1350Hz}$ (%)
1	1.9744	1.1569	0.0198
2	3.6701	4.1668	0.0000
3	13.9131	0.2673	1.1911
4	2.8499	0.3431	0.0228
5	7.5228	0.3165	0.0021
6	5.8565	0.6157	0.0026
7	0.7710	0.7229	0.0078
8	2.0462	0.2574	0.1959
9	1.0617	0.3433	0.0000
10	3.6559	0.7148	0.0220
11	1.4512	40.7501	0.8119
12	1.1849	0.1805	0.0164
13	0.6669	0.0406	0.0007
14	1.2788	0.1240	0.0000
15	0.9802	0.1319	0.0037
16	2.4460	1.3011	0.2550
17	1.9301	0.7024	0.3448
平均值	3.1329	3.0668	0.1704
標準差	3.2416	9.4667	0.3262

表十八.半月板破裂：型態 2-1 的主極點功率比

編號	$R_{300Hz<f<500Hz}$ (%)	$R_{500Hz<f<750Hz}$ (%)	$R_{750Hz<f<1350Hz}$ (%)
1	10.6213	0.5329	0.0299
2	10.2056	1.5268	0.4778
3	1.2186	0.3700	0.0115
平均值	7.3485	0.8099	0.1731
標準差	4.3378	0.5112	0.2156

表十九.半月板破裂：型態 2-2 的主極點功率比

編號	$R_{300Hz<f<500Hz}$ (%)	$R_{500Hz<f<750Hz}$ (%)	$R_{750Hz<f<1350Hz}$ (%)
1	1.7723	19.1367	0.0037
2	5.6292	0.6447	3.4133
3	6.2766	55.6541	0.0159
4	1.5030	0.1573	0.0000
5	4.1543	73.5444	0.0331
平均值	3.8671	29.8274	0.6932
標準差	1.9478	29.7470	1.3601

表二十.半月板破裂：型態 3-2 的主極點功率比

編號	$R_{300Hz<f<500Hz}$ (%)	$R_{500Hz<f<750Hz}$ (%)	$R_{750Hz<f<1350Hz}$ (%)
1	14.6617	5.1606	26.9094
2	0.1801	0.5701	0.0216
平均值	7.4209	2.8653	13.4655
標準差	7.2408	2.2953	13.4439

表二十一.半月板破裂：型態 3-3 的主極點功率比

編號	$R_{300Hz<f<500Hz}$ (%)	$R_{500Hz<f<750Hz}$ (%)	$R_{750Hz<f<1350Hz}$ (%)
1	19.9967	52.7724	1.8119
2	26.9993	7.5373	3.0099
3	10.8492	6.9224	2.9859
4	0.0010	0.0026	0.0000
5	9.0871	28.4387	0.0529
6	17.5235	1.7899	1.4888
7	18.6218	1.2096	19.4328
8	11.0736	0.4166	0.0963
9	12.4300	0.8326	0.0082
10	47.9384	0.1110	0.0023
11	17.9183	3.3357	0.0423
12	8.2265	0.1066	0.0000
13	10.7024	0.0879	38.9865
14	0.3523	0.0682	0.0002
15	2.8445	0.0777	0.0000
16	1.2769	0.5690	76.6631
17	1.9403	0.3273	0.0065
18	1.2798	1.9846	0.2513
19	2.6149	0.3305	1.9900
20	11.3055	3.7095	1.7347
21	5.3036	0.1807	0.0151
22	4.4203	0.2530	1.2863
23	0.5973	0.1186	0.0030
平均值	10.5784	4.8340	6.5160
標準差	10.8058	11.7880	17.2330

Vibration Arthrometry in the Patients with Failed Total Knee Replacement

Ching-Chuan Jiang, Ju-Hong Lee and Tung-Tai Yaun

Reprinted from
IEEE TRANSACTIONS ON BIOMEDICAL ENGINEERING
VOL. 47, NO. 2, JANUARY 2000

Vibration Arthrometry in the Patients with Failed Total Knee Replacement

Ching-Chuan Jiang, Ju-Hong Lee*, and Tung-Tai Yuan

Abstract—**This is a preliminary research on the vibration arthrometry of artificial knee joint *in vivo*. Analyzing the vibration signals measured from the accelerometer on patella, there are two speed protocols in knee kinematics: 1) 2°/s, the signal is called "physiological patellofemoral crepitus (PPC)", and 2) 67°/s, the signal is called "vibration signal in rapid knee motion". The study has collected 14 patients who had revision total knee arthroplasty due to prosthetic wear or malalignment represent the failed total knee replacement (FTKR), and 12 patients who had just undergone the primary total knee arthroplasty in the past two to six months and have currently no knee pain represent the normal total knee replacement (NTKR).**

FTKR is clinically divided into three categories: metal wear, polyethylene wear of the patellar component, and no wear but with prosthesis malalignment. In PPC, the value of root mean square (rms) is used as a parameter; in vibration signals in rapid knee motion, autoregressive modeling is used for adaptive segmentation and extracting the dominant pole of each signal segment to calculate the spectral power ratios in $f < 100$ Hz and $f > 500$ Hz.

It was found that in the case of metal wear, the rms value of PPC signal is far greater than a knee joint with polyethylene wear and without wear, i.e., PPC signal appears only in metal wear. As for vibration signals in rapid knee motion, prominent time-domain vibration signals could be found in the FTKR patients with either polyethylene or metal wear of the patellar component. We also found that for normal knee joint, the spectral power ratio of dominant poles has nearly 80% distribution in $f < 100$ Hz, is between 50% and 70% for knee with polyethylene wear and below 30% for metal wear, whereas in $f > 500$ Hz, spectral power ratio of dominant poles has over 30% disribution in metal wear but only nonsignificant distribution in polyethylene wear, no wear, and normal knee. The results show that vibration signals in rapid knee motion can be used for effectively detecting polyethylene wear of the patellar component in the early stage, while PPC signals can only be used to detect prosthetic metal wear in the late stage.

Index Terms—**Cartilage degeneration, crepitus, failed total knee replacement, knee joint, parametric modeling, patella, vibration arthrometry (VAM).**

I. Introduction

THE human knee joint may produce vibration during flexion-extension motion, which may reflect the internal status of knee structure. In Northern Ireland, Mollan *et al.*. had done a lot of recording, measuring, and analyzing on vibration signals [1]–[7], and used accelerometer instead of microphone for measuring the signals. The accelerometer is smaller in dimension and has better frequency response, while microphone is less sensible to low-frequency signals and more subjective to the surroundings [3]. They found the special signals of meniscal tear and defined the physiological patellofemoral crepitus (PPC) signals [5] for normal knee of human being. In Canada, Rangayyan was devoted to the analysis of VAM signals which are generally nonstationary in nature [8]–[15]. They divided VAM signals into locally stationary signal segments [9]–[11] and extracted parameters, such as autoregressive (AR) coefficients, dominant poles, and cepstral coefficients for classification. The research results of Mollan and Rangnyyan had possibly made VAM a new clinical tool for diagnosis of knee joint disorders.

The cartilage degeneration is a common cause for the aged people who require total knee replacement. Usually, artificial knee joint is composed of three prostheses: femur, tibia, and patella. Femur has a extremely polished alloy metal surface. Tibia has two parts: alloy metal baseplate and ultrahigh molecular weight polyethylene top. Patella is mainly made of polyethylene, some manufacturers produce patella with a metal baseplate. The friction interfaces of knee prosthesis in normal knee movement are the metal part of femur and plastic part of tibia and patella. The two materials have proper stiffness but low surface friction coefficient to each other, can be long lasting if properly implanted. However, wear may occur due to malalignment, accidental collision or material factor, and cause the knee pain. The wear of knee prosthesis will cause particles of ultrahigh molecular weight polyethylene and metal to penetrate into the knee joint cavity, be absorbed by the surrounding tissue and phagocyized. However, the human cells are unable to decompose these particles, which results in rupture and death of the cells, releasing enzymes that will decompose the bone matrix and further cause osteolysis [16]. Metal particles not only subside into the surrounding soft tissue but also circulate to the rest of body through the lymphatic system, which may even be carcinogenic [17].

Currently, two methodologies are adopted for joint diagnosis: invasive and noninvasive. The noninvasive method includes the most popular X-ray and magnetic resonance imaging (MRI). MRI is not able to image metal material, whereas X-ray is merely a one-dimensional projection and unable to reflect plastic material. Therefore, X-ray is only suitable for judging the position of prosthesis but incapable of judging the wear issue. Neither X-ray nor MRI is capable of making accurate diagnosis on prostheic wear in the early stage. The alternative

Manuscript received May 25, 1998; revised August 20, 1999. *Asterisk indicates corresponding author* This work was supported by the National Science Council under Grants NSC87-2314-B002-047 and NSC87-2313-E002-071.

C. C. Jiang is with the Department of Orthopaedic Surgery, National Taiwan University Hospital, Taipei, 100 Taiwan, R.O.C.

*J.-H. Lee is with the Department of Electrical Engineering, National Taiwan University, Room 517, Building 2, Taipei, 106 Taiwan, R.O.C.

T.-T. Yuan is with the Department of Electrical Engineering, National Taiwan University, Taipei, 106 Taiwan, R.O.C.

Publisher Item Identifier S 0018-9294(00)00888-0.

is the arthroscope which is invasive and requires anesthesia for the patient in application, thus more dangerous.

The research motive is to determine whether the VAM can be a new option for diagnosis of prosthetic wear. The hypothesis is that the vibration signals of knee prosthesis in vivo measured by the VAM may be significant for medical use. The purpose is to research and develop a simple, convenient, and cost-saving noninvasive method to provide surgeons a new alternative in diagnosing patients with knee prosthesis wear problems.

II. Materials and Methods

Failed total knee replacement (FTKR) can be divided into metal wear FTKR, plastic wear of the patellar component FTKR, and no wear FTKR but revision required due to prosthetic malalignment. In the study, there are 12 normal total knee replacement (NTKR) and 14 FTKR patients. In the FTKR group, if one of three phenomena, namely clear scratch mark on the metal, metal stain in the joint cavity, or metal particles, is found in the tissue after biopsy, it is called the metal wear FTKR as shown in Fig. 1; if metal part remains smooth but wear appears in the plastic part of the patellar component, it is called plastic wear FTKR; if both metal and plastic parts are intact, it is called no wear FTKR. In the selection of parameters, the rms value of PPC signals is analyzed and AR model is applied to analyze vibration signals in rapid knee motion. In the mean time, adaptive segmentation is performed to make signals locally stationary. Moreover, the spectral power ratio of dominant poles of signal segments is used to differentiate NTKR and FTKR.

A. Research Subject

The research subject is mainly the FTKR patients. The infected prostheses were not included in this study. The total knee prostheses of the 14 FTKR patients included six Tricon (Richard), four PCA modular knee (Howmedica), two PCA primary knee (Howmedica) and two MG I (Zimmer) prostheses. The size of these prostheses were either small or medium. The patellar components of the two MG I prostheses were metal-backed while the patellar components of the remaining 12 prostheses were all polyethylene. The femoral and tibial components of all 14 FTKR patients were noncemented. The patellar components were cemented except the two metal-backed components. All of these 14 total knee prostheses were of cruciate retaining design. In order to see the possibility of VAM to be a diagnostic method for knee wear, it is applied to FTKR patients. Prior to the total knee replacement procedure, VAM is taken from the 14 FTKR patients, cause of FTKR is searched and photographed during the surgery and biopsy is done. The 14 FTKR patients are four males with average age 70 and ten females with average age 67. Time from the primary total knee replacement are five years for male and eight years for female patients in average. On the other hand, 12 patients post-operative between two and six months form the NTKR control group including one male patient aged 64 and 11 female patients with average age 65. VAM is also applied to the NTKR group. All FTKR and NTKR patients are selected from the National Taiwan University Hospital.

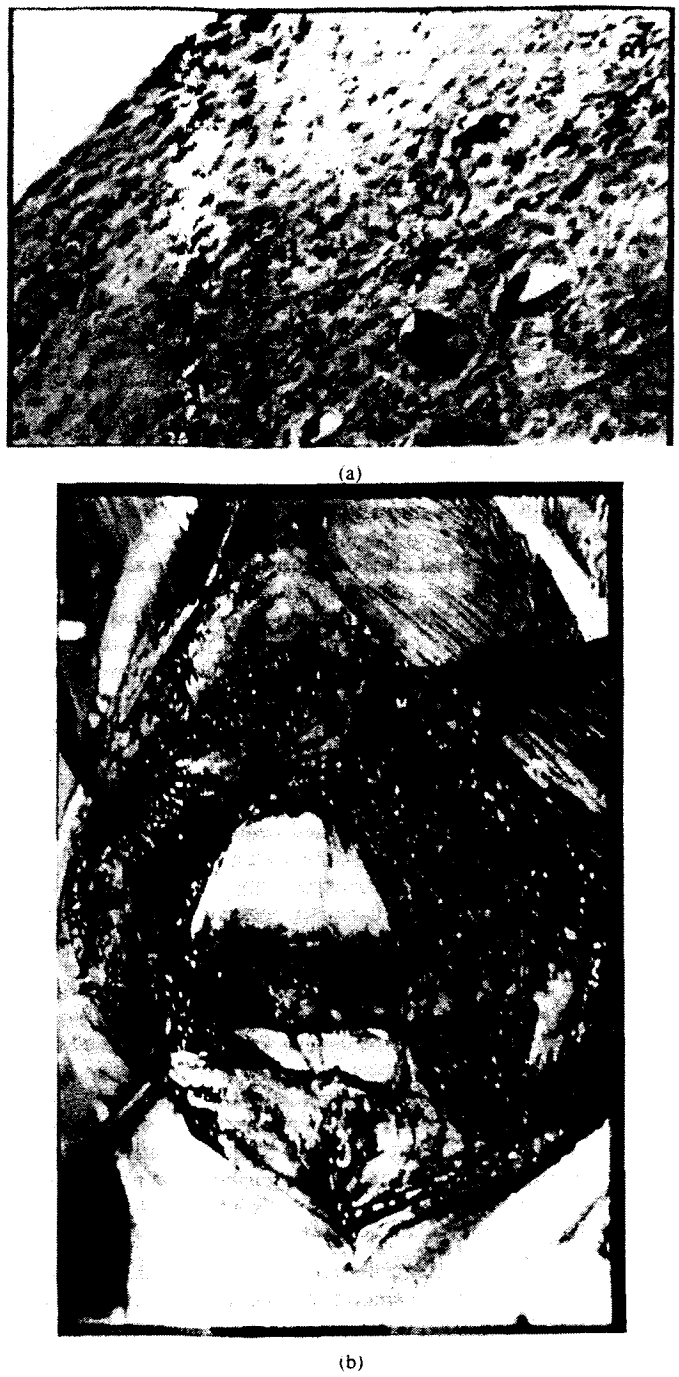

Fig. 1. The photos of metal wear FTKR. (a) The photo of tissue biopsy represents metal particles found in the tissue. (b) The operative findings show metal-stained synovium in the joint cavity.

B. Data Collection

The VAM is collected in two protocols: 1) 2°/s of knee flexion-extension motion, the signal is called "physiology patellofemoral crepitus (PPC)", and 2) 67°/s, the signal is called vibration signal in rapid knee motion. Biodex isokinetic dynamometer (Biodex, New York) is utilized to help the tested patient to swing leg by 2°/s and 67°/s. The procedure is described as follows:

1) Collection of PPC Signals:

Step 1) Record the basic information of the tested patient.

Step 2) Ask the tested patient to take seat on the Biodex chair with knee in natural flexion and feet not touching the ground.
Step 3) Fasten the accelerometer and electrogoniometer.
Step 4) Set the angle of Biodex machine from knee joint extension 0° to flexion 90°.
Step 5) Set the speed of machine to 2°/s.
Step 6) Make sure that the signal cords are properly connected and settings are the same as above. Start the VAM.
Step 7) Advise the tested patient to attach the anterior side of shank closely to the arm pad of the Biodex machine to do extension and flexion of the knee.
Step 8) Turn on the machine. After the tested patient has completed several times of flexion and extension, turn on the personal computer to record the vibration signals.

2) Collection of Vibration Signals in Rapid Knee Motion: The procedure is the same as that of PPC signal except that the velocity in *Step 5* is changed to 67°/s. The choice of this velocity is based on the recommendation of previous authors [11].

A PCB (PCB PIEZOTRONICS, New York) accelerometer (model: 352A22) is positioned on the skin of patella bone center to detect signals [18]. In order to magnify the signal measured, we use the PCB amplifier which is the same brand as accelerometer. The working frequency range is between 0.22 Hz and 100 kHz (±5%). The PCB amplifier is called the preamplifier, followed by AAF-3 anti-aliasing filter (Costa Mesa, CA) which is a low-pass filter with passband equal to 10 kHz. This can avoid the aliasing effect due to high-frequency signal, noise, and interference. Meanwhile, it can also increase signal-to-noise ratio (SNR). The overall gain due to these two amplifiers is 200. We use Bakker BE490 converter (Bakker Electronic, Atlanta, GA) to digitize the vibration signals.

There are two different protocols in this research: For PPC signals, we use sampling rate 5 kHz and 12 bits/sample. For vibration signals in rapid knee motion, we use sampling rate 50 kHz and 12 bits/sample. All analyses are performed on a PC with Pentium CPU. The instrument to record knee angle is electrogoniometer which uses the voltage difference to indicate angle change. Fig. 2 shows the "*assembly*" of the devices measuring signals, while Fig. 3 shows the PPC signals and the vibration signals in rapid knee motion measured from NTKR and FTKR patients.

III. Analysis of Vibration Arthrometry

A. PPC Signal Analysis

The PPC signals are the signals measured when the knee joint goes through a flexion-extension motion slowly at an angular speed of 2°/s. After obtaining the PPC signals for each patient, we compute the root mean square (rms) value of the PPC signals during a complete extension-flexion cycle, i.e., a cycle for swinging movement of the leg from 90° (flexion) to 0° (extension) to 90°. The rms value which is related to the energy content of a PPC signal is given by [19]

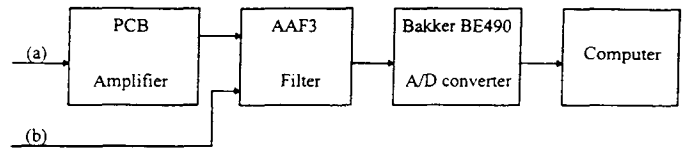

Fig. 2. The system of VAM. (a) The signals measured by accelerometer. (b) The signals measured by electrogoniometer.

$$\text{rms} = \sqrt{\frac{1}{N}\sum_{n=1}^{N} x^2(n)} \tag{1}$$

where $x(n)$, $n = 1, 2, \ldots, N$, are the sample values of the PPC signal and N is the total number of sample points taken during the cycle of slow knee motion. Based on the time-domain waveform and the rms of the recorded PPC signal for each patient, we analyze the state of the knee replacement materials of the patient.

B. Vibration Signals in Rapid Knee Motion

Due to the fact that vibration signals are emitted from the contact and rubbing of the surfaces of knee replacement materials, the vibration signals measured during rapid knee motion may bear diagnostic information about the state of knee replacement materials. Clearly, these signals are nonstationary random signals in nature. Therefore, it is not appropriate to process the signals directly using standard signal processing techniques. However, we can divide the signals into locally stationary segments and then perform a useful signal processing like parametric modeling on the segments. A widely used parametric modeling technique is AR modeling which extracts all linearly retrievable information from the signal optimally in the mean square sense [21].

1) AR Modeling: According to [21], let the signal samples $x(n), x(n-1), x(n-2), \ldots$, represent a realization of the stationary random signal $x(n)$. Based on the theory of AR modeling, we assume that the current signal sample satisfies the following difference equation:

$$x(n) = -\sum_{\ell=1}^{M} a(\ell)x(n-\ell) + w(n) \tag{2}$$

where M is the order of the AR model for the random signal $x(n)$, $a(\ell)$, $\ell = 1, 2, \ldots, M$, are the AR parameters, and $w(n)$ is some input. In the case of knee joint vibration signals, $w(n)$ is totally unknown. Hence, we can approximate the current signal sample by taking the linear combination of its past M samples. From (2), the approximation of $x(n)$ can be given by

$$\hat{x}(n) = -\sum_{\ell=1}^{M} a(\ell)x(n-\ell). \tag{3}$$

It follows from (2) and (3) that the resulting approximation error between $x(n)$ and $\hat{x}(n)$ is given by

$$e(n) = x(n) - \hat{x}(n) = x(n) + \sum_{\ell=1}^{M} a(\ell)x(n-\ell). \quad (4)$$

The corresponding mean squared error for $x(n)$ is the expectation of squared error given by

$$\text{MSE} = E\{|e(n)|^2\}. \quad (5)$$

Hence, the optimum AR parameters can be found by minimizing (5). This leads to solving the Yule–Walker equation given in matrix form as follows [20]: where $\mathrm{r}_{xx}(k) = E\{x^*(n)x(n+k)\}, k = -M+1, \ldots, -1, 0, 1, \ldots, M-1$, are the autocorrelation function of the random signal $x(n)$. Equation (6), shown at the bottom of the page, can be efficiently solved in $O(M^2)$ operations using the Levinson algorithm [22].

From (2), the transfer function $H(z)$ of the AR model is given by

$$H(z) = \frac{1}{1 + \sum_{\ell=1}^{M} a(\ell)z^{-\ell}}. \quad (7)$$

It follows from (7) that the power spectral density (PSD) of the model signal is given by

$$P_m(f) = \left| \frac{1}{1 + \sum_{\ell=1}^{M} a(\ell)e^{-j2\pi f\ell}} \right|^2. \quad (8)$$

For processing and analyzing the vibration signals in rapid knee motion, we utilize the AR modeling technique on each locally stationary segment to find the corresponding AR parameters $a(\ell)$'s from (6). The corresponding PSD for each signal segment is computed from (8) by passing the obtained $a(\ell)$'s through a fast Fourier transform program followed by inversion and squaring.

2) Adaptive Segmentation: Here, the segmentation of vibration signals recorded in rapid knee motion is considered. To achieve the goal of applying conventional signal processing techniques like AR modeling technique, we need to partition the nonstationary vibration signals in rapid knee motion into segments which are stationary. Adaptive segmentation has been successfully used in [9] and [15] for the analysis of nonstationary biomedical signals. Based on the procedure presented in [9], we first estimate the PSD of the signal in a reference window with length N. The PSD is estimated from (8) based on AR modeling. Then, the variations in the PSD spectrum are measured by computing the resulting model error shown by (5). The AR parameters obtained from the reference window are used to model the neighboring window of N points. Finally, the later N points are added to the reference segment if its model error is less than a specified threshold. This procedure is continued until the model error exceeds a specified threshold.

The proposed procedure for adaptive segmentation is summarized step by step as follows.

Step 1) Take the first N points of the recorded signal and find the corresponding AR parameters.

Step 2) Take the next N points of the recorded signal and find the corresponding AR parameters. Using the AR parameters, we compute the resulting model error E_0 as follows [20]:

$$E_0 = \frac{1}{2L+1} \sum_{i=-L}^{L} \frac{P(f_i)}{P_{om}(f_i)}, \quad (9)$$

where f_i, $i = -L, -L+1, \ldots, -1, 0, 1, \ldots, L$, are the frequency grid points uniformly distributed in the frequency range $[-\pi, \pi]$, $2L+1$ is the total frequency points used for computing the PSD. $P(f)$ and $P_{om}(f)$ represent the PSD of the next N points of recorded vibration signal and the PSD of the model signal, respectively.

Step 3) Use the AR parameters obtained from *Step 1* to estimate the N points of the recorded signal in *Step 2*. Then, compute the resulting model error E_1 according to

$$E_1 = \frac{1}{2L+1} \sum_{i=-L}^{L} \frac{P(f_i)}{P_{1m}(f_i)}, \quad (10)$$

where $P_{1m}(f)$ represents the PSD of the signal estimated by the AR parameters of *Step 1*.

Step 4) Compute the ratio $\frac{E_0}{E_1}$. If the ratio $\frac{E_0}{E_1}$ is greater than a preset threshold α, we recognize that these two consecutive N-point signals have similar stationarity. Hence, increase the length of the signal segment by adding the next N points to the segment and go to *Step 2*. If $\frac{E_0}{E_1} \leq \alpha$, a segment boundary is reached. Then, go to *Step 1* to start the procedure again at the next signal sample.

3) Dominant Poles of AR Modeling: The poles of the transfer function $H(z)$ given by (7) contain useful spectral features of the AR model signal. It is well known that the dominant poles for an AR model signal represents the dominant peaks of the signal's PSD. To analyze the vibration signals in rapid knee motion, we utilize the dominant pole that shows the

$$\begin{bmatrix} \mathrm{r}_{xx}(0) & \mathrm{r}_{xx}(-1) & \cdots & \mathrm{r}_{xx}(-M+1) \\ \mathrm{r}_{xx}(1) & \cdot & \cdots & \mathrm{r}_{xx}(-M+2) \\ \cdot & \cdot & \cdots & \cdot \\ \cdot & \cdot & \cdots & \cdot \\ \mathrm{r}_{xx}(M-1) & \cdot & \cdots & \mathrm{r}_{xx}(0) \end{bmatrix} \begin{bmatrix} a(1) \\ a(2) \\ \cdot \\ \cdot \\ a(M) \end{bmatrix} = \begin{bmatrix} \mathrm{r}_{xx}(1) \\ \mathrm{r}_{xx}(2) \\ \cdot \\ \cdot \\ \mathrm{r}_{xx}(M) \end{bmatrix}, \quad (6)$$

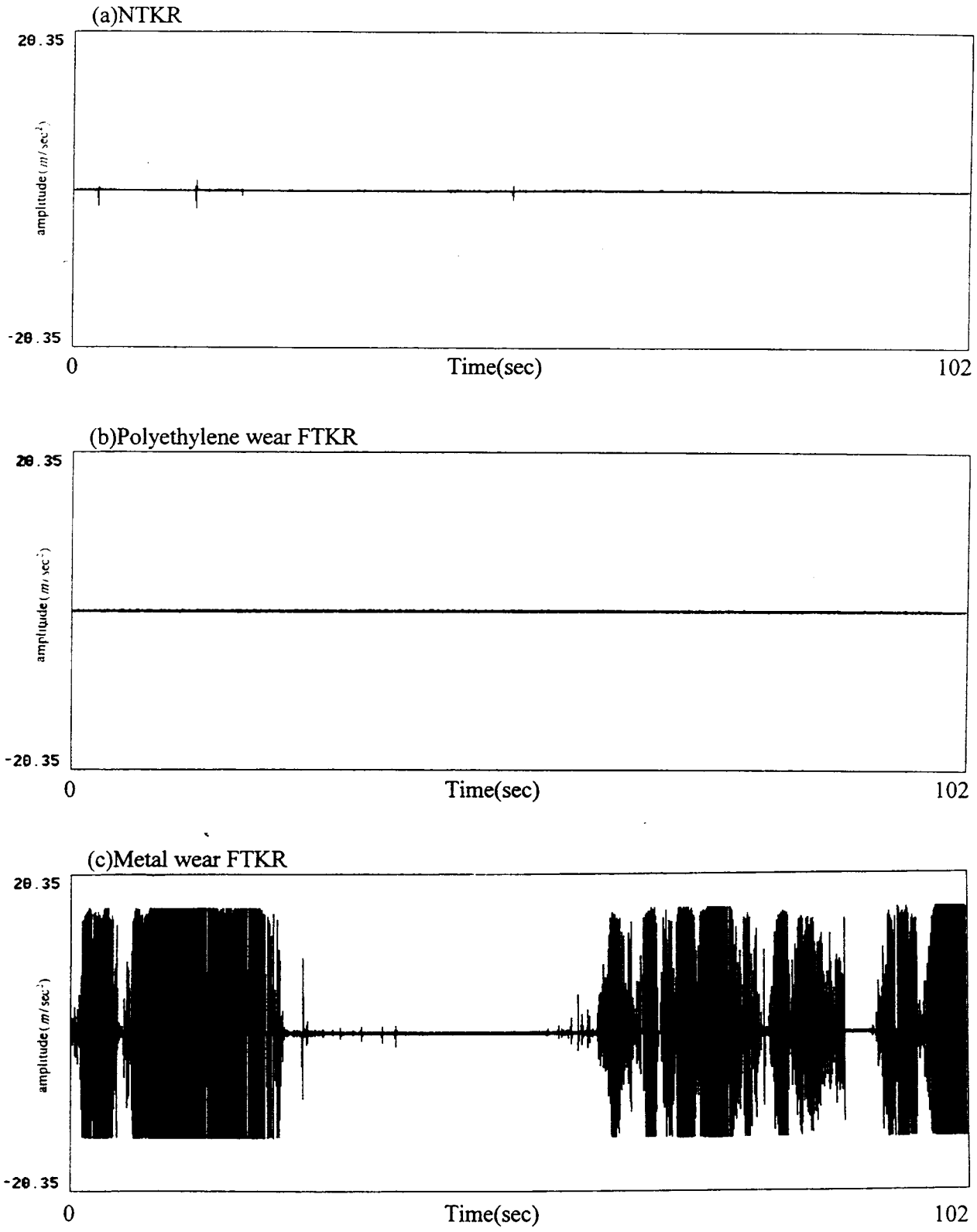

Fig. 3. (a)–(c): The PPC signals for NTKR and FTKR patients.

maximum peak of the PSD. The power of the dominant pole for the kth signal segment is given by

$$\Lambda_k = P_k(f_d) = \max\{P_k(f)\} \tag{11}$$

where $P_k(f)$ denotes the PSD of the kth signal segment and f_d the maximum peak frequency.

4) Spectral Power Ratio of Dominant Poles: For a recorded vibration signal in rapid knee motion, let the number of signal

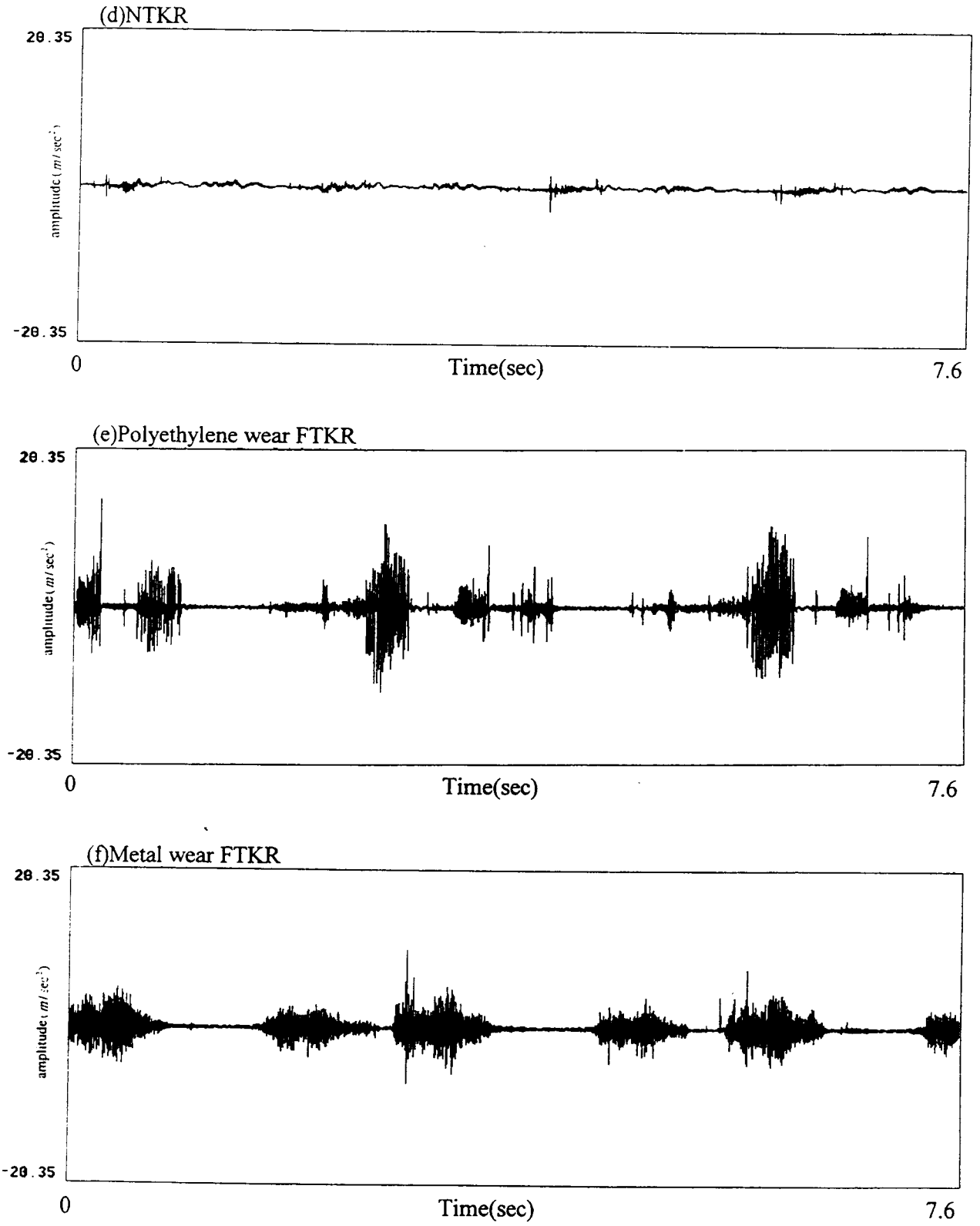

Fig. 3. (*Continued.*) (d)–(f): The vibration signals in rapid knee motion for NTKR and FTKR patients.

segments after performing adaptive segmentation be K and the total power of the kth segment be P_k. Then, we have

$$P_k = \sum_{f_i} P_k(f_i), \quad k = 1, 2, \ldots, K \tag{12}$$

and the average segment power of the recorded vibration signal is given by

$$\bar{P} = \frac{1}{K} \sum_{k=1}^{K} P_k. \tag{13}$$

From the data collection described in Section II-B, the amount of signal samples for each patient is over one hundred thousands. After adaptive segmentation, the number of segments is in general about several hundreds. However, some of the signal segments may possess very small total power and, hence, do not bear useful information for analysis. Accordingly, it is appropriate to consider only the signal segments with total power not less than a suitable threshold. To find the suitable threshold, we perform the similar AR modeling and adaptive segmentation on the vibration signals recorded from the patients with NTKR. Let the average segment power for the signal measured from the kth patient be $\bar{P}_{Nk}, k = 1, 2, \ldots$, the threshold can be set to

$$T = \frac{1}{J} \sum_{k=1}^{J} \bar{P}_{Nk} \tag{14}$$

where J is the number of patients with NTKR.

Assume that there are n_T signal segments with segment power not less than the threshold T. The power of the most dominant pole, $\Lambda_k, k = 1, 2, \ldots, n_T$, and the corresponding maximum peak frequency f_d for each of the signal segments are computed by using (11). Then, we define the spectral power ratio of dominant poles for a recorded vibration signal as follows:

$$R_{f_1 < f_d < f_2} = \frac{\sum_{k \in \mathbf{G}} \Lambda_k}{\sum_{k=1}^{n_T} \Lambda_k} \tag{15}$$

where **G** represents the set of the subscripts k for which the corresponding kth signal segment has f_d between f_1 and f_2. From (15), we note that $R_{f_1 < f_d < f_2}$ is a measure regarding the power concentration of a vibration signal in the frequency band (f_1, f_2). From our study of the vibration signals in rapid knee motion, it is observed that the power concentrations for patients with different states of knee replacement materials demonstrate significant distinctions. Therefore, we use the spectral power ratio of dominant poles for analyzing the vibration signals in rapid knee motion.

IV. Results

A. Clinical Findings

The study has collected 14 FTKR patients as an experimental group for evaluating the wear situation of the prosthesis which are removed in surgery. We have found that the polyethylene part of patella has worn out in two of the 14 FTKR cases. This results in the metal-back of patellar component exposed to contact with femoral component. The metal particles in tissue are found through pathological biopsy. This is mainly caused by metal to metal wear. There are patellar polyethylene wear being observed in eight of 14 FTKR cases. The surface of patella is no longer smooth. The last four FTKR cases have no wear situation occurred. The reason of revision is due to malalignment of the prosthesis. Bony ingrowth was found in all the porous coated surfaces of the tibial and femoral components of the 14 retrieved total knee prostheses. No radiological evidence of implant loosening was found in these patients. Various degrees of patellar subluxation were demonstrated by Merchant's view radiographs in two metal-wear and eight polyethylene-wear patients. For the NTKR control group consisting of 12 NTKR patients, they were all postoperative in between two and six months. Although the surface of prostheses cannot be directly evaluated, we have found from the X-ray that the size of the prosthesis chosen and the location of prosthesis placed are correct. The patients are symptom free and are recovering well.

TABLE I
THE RMS VALUES FOR ALL NTKR AND FTKR PATIENTS

The patient number of FTKR		$RMS\left(m/sec^2\right)$	The patient number of NTKR	$RMS\left(m/sec^2\right)$
metal	1	0.5860	1	0.0473
metal	2	1.7200	2	0.0318
polyethylene	1	0.0376	3	0.0365
polyethylene	2	0.0479	4	0.0385
polyethylene	3	0.0366	5	0.0386
polyethylene	4	0.0367	6	0.0414
polyethylene	5	0.0427	7	0.0579
polyethylene	6	0.0374	8	0.0458
polyethylene	7	0.0413	9	0.0322
polyethylene	8	0.0533	10	0.0462
no wear	1	0.0595	11	0.1319
no wear	2	0.0468	12	0.0314
no wear	3	0.0463		
no wear	4	0.0513		

B. Analysis of PPC Signals

On the speed of 2°/s to detect the vibration signals, there are no PPC signals produced in NTKR control group, patellar polyethylene wear of eight FTKR's, and no wear of four FTKR's as shown in Fig. 3(a) and (b). Only the metal wear of FTKR has caused PPC signals as shown in Fig. 3(c). Table I lists the rms value of PPC signals for the NTKR control group. The mean value is 0:0483. The standard deviation (SD) is 0.0274. The rms values of the eight patellar polyethylene wear FTKR's and the four no wear FTKR's are close to those of the NTKR control group. In contrast, the rms values of the two metal wear FTKR's are 0.586 and 1.72.

C. Analysis of Vibration Signals in Rapid Knee Motion

When knee joint movement is on the speed of 67°/s, the signals measured are called vibration signals in rapid knee motion. Accelerometer is placed on patella to measure the vibration signals. In this study, the average segment power threshold T of the NTKR control group is 0.0177. The SD is 0.0064. When a signal segment has power greater than 0.0177, it is viewed as a useful signal segment for analysis. The α value is 0.85 according to [9]. After trying many different frequency bands of spectral power ratio of dominant poles, we have found that $R_{f_d < 100}$ is almost close to or more than 80% distribution in the NTKR control group as shown in Table II. In Table III, $R_{f_d < 100}$ is greater than 80% for the no wear FTKR group and is lower than 30% for the metal wear FTKR group. In contrast, $R_{f_d} < 100$ is between 50% and 70% for the polyethylene wear FTKR group. When $R_{f_d > 500}$, there is high percentage distribution found in the metal

TABLE II
THE SPECTRAL POWER RATIOS OF DOMINANT POLES FOR NTKR PATIENTS

The patient number of NTKR	$R_{f_d<100}$	$R_{f_d>500}$
1	80.90%	4.38%
2	78.29%	5.25%
3	81.29%	6.41%
4	80.70%	2.93%
5	80.49%	12.79%
6	79.33%	1.72%
7	76.28%	3.83%
8	77.60%	4.69%
9	81.83%	8.76%
10	85.03%	0.71%
11	77.33%	2.51%
12	80.07%	9.09%

TABLE III
THE SPECTRAL POWER RATIOS OF DOMINANT POLES FOR FTKR PATIENTS

The patient number of FTKR		$R_{f_d<100}$	$R_{f_d>500}$
metal	1	19.22	33.13%
metal	2	25.29%	48.33%
polyethylene	1	61.27%	12.78%
polyethylene	2	67.18%	8.18%
polyethylene	3	56.11%	3.00%
polyethylene	4	57.08%	5.84%
polyethylene	5	66.38%	8.23%
polyethylene	6	64.35%	27.10%
polyethylene	7	54.89%	19.37%
polyethylene	8	61.70%	0 %
no wear	1	84.63%	7.56%
no wear	2	91.05%	0.88%
no wear	3	86.57%	3.66%
no wear	4	81.84%	5.79%

wear FTKR group, for example, the percentages of two metal wear FTKR's are 33.13% and 48.33%. However, there are no significant distributions found in the NTKR group, the polyethylene wear FTKR group, and the no wear FTKR group.

From the distributions of $R_{f_d<100}$ and $R_{f_d>500}$, we observe that in the range of $f_d < 100$ Hz, the NTKR control group has higher distribution and the no wear FTKR group has similar result as that of the NTKR control group, the polyethylene wear FTKR group is the second, and the metal wear FTKR group has the lowest distribution. In contrast, for the range of $f_d > 500$ Hz, the metal wear FTKR group has significantly higher distribution than those of the polyethylene wear FTKR group, the no wear FTKR group, and the NTKR control group.

V. DISCUSSION AND CONCLUSION

About the VAM of artificial knee joint *in vivo*, so far, there is no related reference reported. The study is the first one being brought out. Due to the shortage of cases, the current results are still not enough to establish statistical significance. It will need more cases to support the correctness of the obtained results. From the study, we have found that PPC signals are only detected in two cases of the metal wear FTKR group. All of the NTKR control group, the polyethylene wear FTKR group, and the no wear FTKR group have no PPC signals produced. The production of PPC signals is caused by stick and slip phenomenon when the contacting surfaces of two objects are sliding with each other. The femoral component of knee prosthesis is made of metal material with the characteristics of smooth surface and low friction coefficient. Patellar component is mainly made of high molecular weight polyethylene. There are two types of patellar component, one is all-poly and the other is metal-back. We assume when the polyethylene of patellar component is worn-out, and the metal-back is exposed, the metal-back of patellar component could contact with femoral component in which the situation destroys the smooth surface of metal and causes "stick and slip phenomenon". Before the metal-back of patellar component is exposed, there is no "stick and slip phenomenon". Therefore, PPC signals can only be utilized to judge whether there is metal wear in knee prosthesis, but can not be used for the detection of polyethylene wear in the early stage. When the PPC signals occur, it means that metal wear already exists. Although not many metal-backed patellar components are currently being implanted and metal wear detection may not be important in the future, the VAM is still a good diagnostic tool for the detection of metal wear in those patients already implanted with metal-backed patellar prostheses.

Although prominent vibration signals could be detected during rapid knee motion in the FTKR patients with either polyethylene wear or metal wear as shown by Fig. 3(e) and (f), the vibration signals in rapid knee motion are nonstationary in nature. For not being able to use standard signals processing technique for analysis, we have performed adaptive segmentation to convert them into locally stationary signal segments. After trying different frequency bands of spectral power ratio of dominant poles, we have observed that the spectral power ratio has high percentage distribution for $f_d > 500$ Hz and has the lowest percentage distribution for $f_d < 100$ Hz in the two cases of metal wear FTKR group. This particular phenomenon only exists in the metal wear FTKR group. For the NTKR control group, the spectral power ratios are almost close to or higher than 80% in distribution in the range of $f_d < 100$ Hz. In the eight cases of patellar polyethylene wear FTKR group, the spectral power ratios are all smaller than 70% in the range of $f_d < 100$ Hz. The result of the the four cases of no wear FTKR group is close to that the NTKR control group when $f_d < 100$ Hz. The cause of revision is the prosthesis placed in varus. Therefore, the application of vibration signals in rapid knee motion can provide early detection to the polyethylene wear of the patellar component. When the wear of prosthetic joint can be detected, we are able to provide a conservative treatment. All the eight patients with patellar polyethylene wear had patello-femoral maltracking. Eccentric patello-femoral contact (usually on lateral facet of the patellar component) could increase patello-femoral contact pressure locally and will enhance polyethylene wear problem. Once polyethylene wear could be detected earlier, we can take action to study the patello-femoral tracking. In dealing with patellar subluxation, either some conservative treatments could be prescribed, e.g.,

knee bracing, quadriceps muscle training, or surgical interventions, e.g., lateral retinacular release, patellar realignment procedures could bring the patellar component back to a normal tracking, so that further polyethylene wearing on the patellar component could be prevented. Thus, the proposed method can prevent the wear to be more aggressive and, hence, could prevent the need of revision knee arthroplasty afterward.

The study mainly concentrates on the patellofemoral joint surface. About the femur-tibia joint surface, we need to place the accelerometer on the medial side or the lateral side of tibial tubercle to analyze vibration signals. According to the result obtained in this paper, VAM may provide surgeons a new alternative in diagnosing patients with knee prosthesis wear problems.

REFERENCES

[1] R. A. B. Mollan, G. C. McCullagh, and R. I. Wilson, "A critical appraisal of auscultation of human joints," *Clin. Orthopaed. Related Res.*, vol. 170, pp. 231–237, Oct. 1982.

[2] W. G. Kernohan, D. E. Beverland, G. F. McCoy, S. N. Shaw, R. G. H. Wallace, G. C. McCullagh, and R. A. B. Mollan, "The diagnostic potential of vibration arthrography," *Clin. Orthopaed. Related Res.*, pp. 106–112, Sept. 1986.

[3] W. G. Kernohan and R. A. B. Mollan, "Microcomputer analysis of joint vibration," *J. Microcomputer Appl.*, vol. 5, pp. 287–296, 1982.

[4] D. E. Beverland, G. F. McCoy, W. G. Kernohan, and R. A. B. Mollan, "What is patellofemoral crepitus?," *J. Bone Joint Surg.*, vol. 68-B, p. 496, Mar. 1986.

[5] G. F. McCoy, J. D. McCrea, D. E. Beverland, W. G. Kernohan, and R. A. B. Mollan, "Vibration arthrography as a diagnostic aid in diseases of the knee," *J. Bone Joint Surg.*, vol. 69-B, no. 2, pp. 288–293, Mar. 1987.

[6] G. F. McCoy, D. E. Beverland, W. G. Kernohan, A. Agahi, and R. A. B. Mollan, "Vibration arthrography in knee joint disease," presented at the 8th Combined Meeting of Orthopaedic Association of the English-Speaking World and The American Orthopaedic Association, Washington, DC, May 1987.

[7] W. G. Kernohan, D. E. Beverland, G. F. McCoy, A. Hamilton, P. Watson, and R. A. B. Mollan, "Vibration arthrometry," *Acta. Orthop. Scand.*, pp. 70–79, 1990.

[8] C. B. Frank, R. M. Rangayyan, and G. D. Bell, "Analysis of knee joint sound signals for noninvasive diagnosis of cartilage pathology," *IEEE Eng. Med. Biol. Mag.*, pp. 65–68, 1990.

[9] S. Tavathia, R. M. Rangayyan, C. B. Frank, G. D. Bell, K. O. Ladly, and Y. T. Zhang, "Analysis of knee vibration signals using linear prediction," *IEEE Trans. Biomed. Eng.*, vol. 39, pp. 959–970, Sept. 1992.

[10] Z. M. K. Moussavi, R. M. Rangayyan, G. D. Bell, C. B. Frank, K. O. Ladly, and Y. T. Zhang, "Screening of vibroarthrographic signals via adaptive segmentation and linear prediction modeling," *IEEE Trans. Biomed. Eng.*, vol. 43, pp. 15–23, Jan. 1996.

[11] S. Krishnan, R. M. Rangayyan, G. D. Bell, C. B. Frank, and K. O. Ladly, "Recursive least squares-lattice based adaptive segmentation, and autoregressive modeling of nonstationary vibroarthrography signals," in *Proc. Canadian Conf. Electrical and Computer Engineering*, Calgary, Alta., Canada, May 1996, pp. 339–342.

[12] Y. T. Zhang, C. B. Frank, R. M. Rangayyan, and G. D. Bell, "Mathematical modeling and spectrum analysis of the physiological patello-femoral pulse train produced by slow knee movement," *IEEE Trans. Biomed. Eng.*, vol. 39, pp. 971–979, Sept. 1992.

[13] Y. T. Zhang, R. M. Rangayyan, C. B. Frank, and G. D. Bell, "Adaptive cancellation of muscle contraction interference from knee joint vibration signals," *IEEE Trans. Biomed. Eng.*, vol. 41, pp. 181–191, Feb. 1994.

[14] R. M. Rangayyan, S. Krishnan, G. D. Bell, C. B. Frank, and K. O. Ladly, "Impact on muscle contraction interference cancellation on vibroarthrographic screening," in *Proc. Int. Conf. Biomedical Engineering*, Kowloon, Hong Kong, June 1996, pp. 16–19.

[15] ——, "Parametric representation and screening of knee joint vibroarthrographic signals," *IEEE Trans. Biomed. Eng.*, vol. 44, pp. 1068–1074, Nov. 1997.

[16] T. S. Thornhill and J. H. Maquire, "Infected total knee arthroplasty," in *Total Knee Revision Arthroplasty*, W. N. Scott, Ed. New York: Grune & Stratton, 1987.

[17] D. D. Goetz, E. J. Smith, and W. H. Harris, "The prevalence of femoral osteolysis associated with components inserted with or without cement in total hip replacements," *J. Bone Surg.*, vol. 76-A, no. 8, pp. 1121–1129, Aug. 1994.

[18] C.-C. Jiang, Y.-J. Liu, K.-M. Yip, and E. Wu, "Physiological patellofemoral crepitus in knee joint disorders," *Bull. Hospital for Joint Diseases*, vol. 53, pp. 7–12, 1994.

[19] S. C. Chapra and R. P. Canale, *Numerical Methods for Engineers*. New York: McGraw-Hill, 1989.

[20] J. Makhoul, "Linear prediction: A tutorial review," *Proc. IEEE*, vol. 63, pp. 561–580, Apr. 1975.

[21] S. Haykin, *Adaptive Filter Theory*, 3rd ed. Englewood Cliffs, N.J.: Prentice-Hall, 1996.

[22] S. M. Kay, *Modern Spectral Estimation*. Englewood Cliffs, N.J.: Prentice-Hall, 1988.

Ching-Chuan Jiang was born in Changhwa, Taiwan, R.O.C. on August 5, 1951. He received the Ph.D. degree from the school of medicine, National Taiwan University, Taipei, Taiwan, R.O.C.

He is a Professor in the Department of Orthopaedic Surgery, National Taiwan University and the Director of Division of Sports Medicine, National Taiwan University Hospital, Taiwan, R.O.C.

Dr. Jiang is a member of Orthopaedic Research Society, American Society of Biomechanics and American Orthopaedic Society of Sports Medicine, and the Chairman of the Arthroscopy and Knee Association, Taiwan, R.O.C.

Ju-Hong Lee was born in I-Lan, Taiwan, R.O.C. on December 7, 1952. He received the B.S. degree from the National Cheng-Kung University, Tainan, Taiwan, R.O.C., in 1975, the M.S. Degree from the National Taiwan University, Taipei, Taiwan, R.O.C., in 1977, and the Ph.D. degree from Rensselaer Polytechnic Institute, Troy, NY, in 1984, all in electrical engineering.

From September 1980 to July 1984, he was a Research Assistant and was involved in research on multidimensional recursive digital filtering in the Department of Electrical, Computer, and Systems Engineering at Rensselaer Polytechnic Institute. From August 1984 to July 1986, he was a Visiting Associate Professor and later in August 1986 became an Associate Professor in the Department of Electrical Engineering, National Taiwan University. Since August 1989, he has been a Professor at the same university. He was appointed Visiting Professor in the Department of Computer Science and Electrical Engineering, University of Maryland, Baltimore, during a sabbatical leave in 1996. His current research interests include multidimensional digital signal processing, image processing, detection and estimation theory, analysis and processing of joint vibration signals for the diagnosis of cartilage pathology, and adaptive signal processing and its applications in communications.

Dr. Lee received Outstanding Research Awards from the National Science Council (NSC) in the academic years of 1988, 1989, and 1991–1994, and a Distinguished Research Award from the NSC in the academic year of 1998.

Tung-Tai Yuan was born in Taichung, Taiwan, R.O.C., on March 18, 1970. He received the B.S. degree from the National Sun Yat-Sen University, Kaohsiung, Taiwan, R.O.C., in 1993 and the M.S. degree from the National Taiwan University, Taipei, Taiwan, R.O.C., in 1998, all in electrical engineering.

His research interests include digital signal processing and its applications.